American Mineralogist, Volume 89, pages 1330–1336, 2004

Ultra-deep origin of garnet peridotite from the North Qaidam ultrahigh-pressure belt, Northern Tibetan Plateau, NW China

SHUGUANG SONG,[1] LIFEI ZHANG,[1,*] AND YAOLING NIU[2]

[1]MOE Key Laboratory of Orogenic Belts and Crustal Evolution, School of Earth and Space Sciences, Peking University, Beijing 100871, China
[2]Department of Geosciences, University of Houston, Houston, Texas 77204, U.S.A.

ABSTRACT

Exsolution textures are observed in garnet and olivine crystals found in an orogenic garnet peridotite massif in the North Qaidam ultrahigh-pressure metamorphic (UHP) belt, northern Tibetan Plateau, NW China. Exsolutions in garnet consist of densely packed rods of rutile, orthopyroxene, and clinopyroxene. Exsolutions in olivine includes needles of ilmenite and Al-chromite. The occurrence of pyroxene exsolution lamellae in garnet crystals suggests that the precursor phase originally must have possessed excess Si, i.e., they were majoritic garnets that are stable only at very high pressures. The exsolution of ilmenite and Al-chromite needles from olivine is also consistent with the peridotite once being equilibrated at depths in excess of 200 km. Geotheromobarometric calculations using matrix minerals of the peridotite yield re-equilibrium conditions of T = 960–1040 °C and P = 5.0–6.5 GPa. These observations and inferences, together with other petrological data and field observations, allow us to conclude that the garnet peridotite in the North Qaidam UHP belt may represent mantle materials exhumed form depths of greater than 200 km.

INTRODUCTION

Orogenic garnet peridotites that occur as lenses associated with eclogites and other high-grade crustal rocks are volumetrically minor but tectonically significant components within many ultrahigh-pressure (UHP) metamorphic terranes. Their ubiquitous occurrences within orogenic belts as a result of continental collision (Medaris and Carswell 1990) and their deep origin (>6 GPa) in some UHP terranes such as Dabie-Sulu of China (Yang et al. 1993; Zhang R.Y. 2000), Western Gneiss Region of Norway (van Roermund and Drury 1998; van Roermund et al. 2000, 2002), Granulitgebirge of Germany (Massonne and Bautsch 2002), and Alpe Arami of Italy (Dobrzhinetskaya et al. 1996; Green et al. 1997; Bozhilov et al. 1999) offer us a prime opportunity for a better understanding of geodynamic processes of continental collision, subduction, and exhumation both on a regional scale and in a global context. Garnet peridotites of this kind have, therefore, received much attention in recent years (e.g., Liou and Carswell 2000).

It is not straightforward, however, to identify precisely the original environment in which these peridotites were formed and to determine accurately the primary conditions under which they may have been equilibrated. This difficulty is because orogenic peridotites are likely to have experienced complex equilibration histories, and because they often lack pressure index minerals such as coesite, diamond, etc. several model geothermometers and geobarometers are available for peridotite systems in the literature, but uncertainties can be very large in these models (e.g., see Smith 1999 for a review). Even if these thermobarometers are reliable, their estimated temperatures and pressures are likely to be minimum values because these peridotites must have experienced prolonged decompression and cooling histories during exhumation. In this case, exsolution textures, if preserved in the constituent minerals of these rocks, are valuable, and can provide useful information on both the environment in which these rocks might be originated and primary physical conditions under which these rocks may have been equilibrated. Exsolution lamellae are fine crystals that were dissolved entirely in their host mineral structures at high temperatures (e.g., clino- and ortho-pyroxenes) and pressures (e.g., majorite-pyroxenes) during formation, but are produced when their host minerals lose the solubility as a result of cooling to low temperatures or decompression to low pressures (for summary, see Zhang and Liou 1999).

In this contribution, we report petrology and exsolution textures observed in the constituent garnet and olivine crystals of an orogenic garnet peridotite from the Luliangshan area of the North Qaidam Basin, northern Tibetan Plateau (Fig. 1A). The garnet peridotite, which was described as a kimberlitic ultramafic body by Bureau of Geology and Mineral Resources of Qinghai Province (1991) and then recognized by Yang et al. (1994), occurs as several large lensoid blocks in an area of 500×1000 m^2 within quartzofeldspathic gneisses (Figs. 1B and 1C). In fact, this garnet peridotite body is a member of a newly recognized ultrahigh-pressure (UHP) metamorphic belt (Song 2001; Yang et al. 2002; Song et al. 2003a). Our observed exsolution textures, along with other lines of evidence, allow us to conclude that the garnet peridotite may represent materials exhumed from depths in excess of 200 km during a continental collision event in the early Paleozoic (495 ± 7 Ma by U-Pb single zircon method, Zhang J.X. 2000; 459 ± 2.6 and 458 ± 10 Ma by Sm-Nd internal isochron method, Song et al. 2003b). These observations also offer implications for the regional tectonic evolution in particular

* E-mail: lfzhang@pku.edu.cn

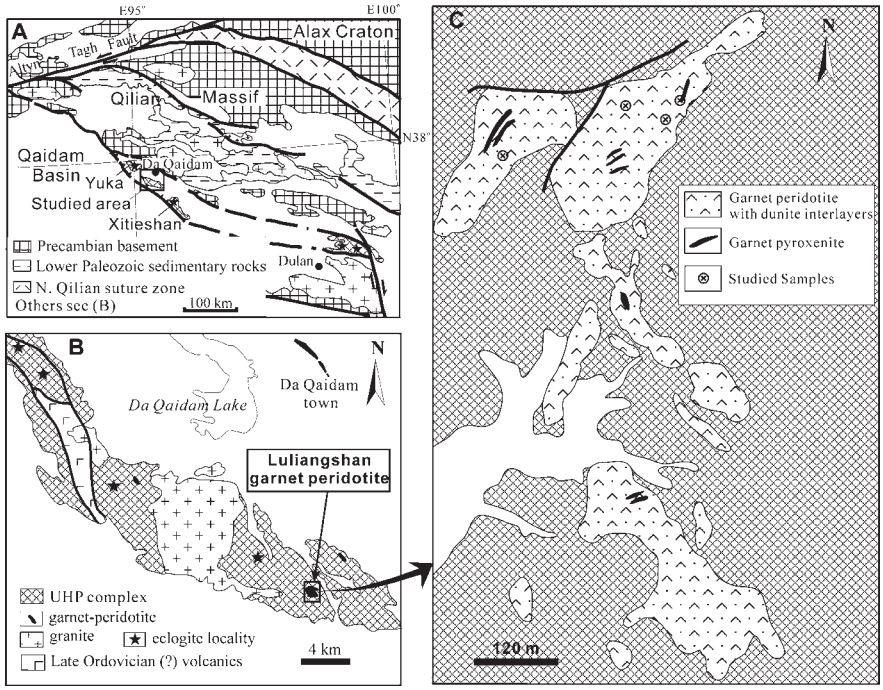

FIGURE 1. (**A**) Geological map of the North Qaidam UHP belt and adjacent areas showing the tectonic units in the North Tibetan Plateau, NW China. (**B**) Geological map showing the locality of the Luliangshan garnet peridotite body. (**C**) Geological map of the garnet peridotite showing locations of the studied samples (modified after Bureau of Geology and Mineral Resources of Qinghai Province 1991).

in the Earth's mantle in general in the context of geochemical recycling.

GEOLOGICAL SETTING

The North Qaidam UHP belt extends from Dulan northwestward through Xietieshan and Luliangshan, to Yuka for about 400 km (see Fig. 1A for localities). To the south is the Qaidam Basin, a Mesozoic intra-continental basin with a Precambrian crystalline basement. To the north is the Qilian Terrain consisting of an imbricate thrust belt of Precambrian basement with thick Paleozoic sedimentary sequences. The Qilian Terrain is bound further to the north by an Early Paleozoic Pacific-type suture following the definition of Ernst (2001) with well-exposed blueschists and ophiolites (Wu et al. 1993; Song 1996).

The Luliangshan garnet peridotite is the largest outcrop recognized so far along the entire Qaidam UHP Belt. As shown in Figure 1C, it occurs as blocks of various sizes in an exposed area of about 500×1000 m^2 within felsic gneisses. Three rock types are recognized in the field. Garnet peridotite comprises about 80 vol% of the body. As clinopyroxene varies in abundance on various scales, the peridotite could be termed a garnet harzburgite or lherzolite (see below). Dunite (with or without garnet) (~15 vol%) and garnet pyroxenite (<5 vol%) make up the rest of the rock body. Garnet peridotite and dunite apparently are interlayered on different scales determined by relative abundances of olivine and pyroxene. Such layering could well be inherited from primary igneous layering such as seen in layered cumulates, but could also be of metamorphic origin. Detailed petrology and geochemistry is needed for a better understanding of the origin of the layering. Garnet pyroxenite occurs as veins and crosscuts the apparent garnet peridotite layering (Fig. 1C). No eclogite was found within the peridotite body.

SAMPLE PETROLOGY

Garnet peridotite

Garnet peridotite consists of garnet (~10–20 vol%), olivine (~40–60 vol%), orthopyroxene (~15–25 vol%), clinopyroxene (~5–15 vol%), and minor amounts of Cr-rich spinel, and shows a coarse-grained granoblastic texture. Most garnet crystals are porphyroblastic with varying grain size (3–10 mm) (Fig. 2a) and few are poikiloblastic (1–2 mm) within the matrix. Almost all the garnet crystals exhibit kelyphitized rims of clinopyroxene, orthopyroxene, and spinel aggregates interpreted as resulting from decompression (Fig. 2a). In some samples, some garnet grains are replaced completely by the kelyphitic Opx + Cpx + Spl assemblage. Electron probe microanalysis shows that these garnets are Mg-Cr type with ~61–74 mol% pyrope, ~15–23 mol% almandine (+ spessartine), ~1.8–9.4 mol% uvarovite, ~0–4 mol% andradite, and ~ 4.2–6.6 mol% grossular. Most olivine crystals are, to various extents, serpentinized. However, their original crystal shapes (mostly anhedral), grain size (0.2–2 mm), and modes (20–60 vol%) are readily determined. Based on texture and grain size, olivine can be divided into two generations: the first generation is coarse-grained (>0.5 mm), and is in equilibrium with coarse-grained garnet and the two pyroxenes (Fig. 2b), whereas the second generation olivine is usually fine-grained and fills the interstices of the first generation minerals. Electron probe microanalysis shows that both generations of olivine in the studied samples is very magnesian with a narrow compositional range ($Fo_{90\text{-}91}$). Cr-rich spinel occurs as fine-grained (5–100 μm) euhedral crystals scattered fairly uniformly both in-between and as inclusions in major silicate minerals; they are clearly the products of breakdown or exsolution of Cr-rich pyroxene and olivine. We thus infer that these spinels are secondary and are not in equilibrium with garnet +

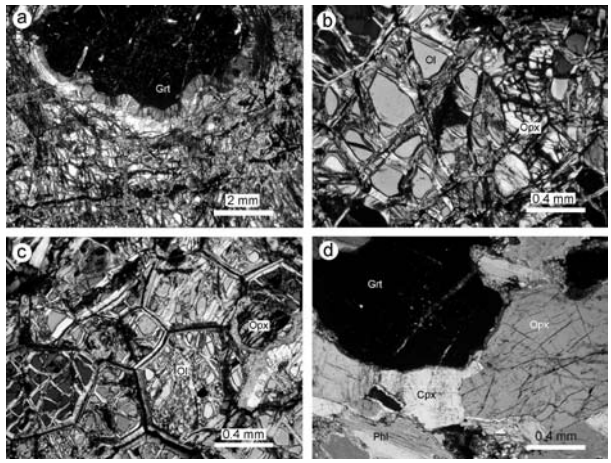

FIGURE 2. Photomicrographs showing textures and mineral assemblages in various rocks in the Luliangshan garnet peridotite body. All are in cross-polarized, transmitted light. (**a**) Garnet lherzolite (2C28) with porphyroblastic garnet; note the exsolution rods in garnet. (**b**) Garnet lherzolite (2C42) showing the first generation of coarse-grained olivine with exsolution rods. (**c**) Dunite (2C39) showing polygonal texture with 120° triple junctions. (**d**) Garnet pyroxenite with mineral assemblage of Grt + Opx + Cpx + Phl. Mineral abbreviations are after Kretz (1983).

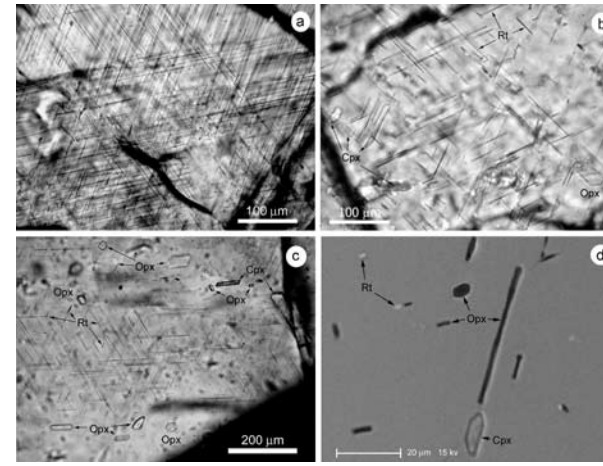

FIGURE 3. Photomicrographs showing rutile, orthopyroxene and clinopyroxene exsolutions in garnets from garnet peridotite. (**a**) Densely packed rutile lamellae in garnet from Sample 2C42. Note the equilateral triangle patterns defined by the exsolution needles (plane-polarized transmitted light). (**b**) Ortho- and clinopyroxene lamellae in garnet from sample 2C28 (plane-polarized transmitted light). (**c**) Hexagonal prismatic basal sections of pyroxene lamellae in company with rutile needles in garnet from sample 2C42 (plane-polarized transmitted light). (**d**) BSE image of ortho- and clinopyroxene exsolutions in garnet from sample 2C28.

pyroxene + olivine of peak conditions. The Cr′ [Cr/(Cr+Al)] of spinel is in the range 0.61–0.70.

Dunite

Dunite is dominated by olivine (up to 95 vol%) with minor amounts of garnet (0–3%) and two types of pyroxene (2–5%). Most garnet crystals are porphyroblastic and Mg-rich with 69–75 mol% pyrope, 11–18% almandine, 3–8% grossular, 0.8–2.0% spessartine, and 3–6% uvarovite. Olivine in the dunite shows a homogeneous granoblastic texture with triple 120° junctions (Fig. 2c), ranging from 0.5 to 1 mm in size. It contains slightly higher Fo (Fo_{92-93}) than in the garnet peridotite.

Garnet pyroxenite

Garnet pyroxenite is a minor component and occurs as dikes 2–5 m in thickness cross-cutting the layering of the massif. The constituent phases are garnet (20–30 vol%), orthopyroxene (5–10%), clinopyroxene (40–60%) and phlogopite (2–5%) with no olivine observed (Fig. 2d). Garnets are also Mg-rich with 62–68 mol% pyrope, 21–24% almandine, 9.5–11% grossular, <1% spessartine, and 0.8–1.5% uvarovite. En content of orthopyroxene ranges from 84 to 87 mol%, lower than that of orthopyroxene in garnet lherzolite/harzburgite and dunite.

EXSOLUTION LAMELLAE IN GARNET

Three different varieties of exsolution lamellae are recognized in garnet porphyroblasts of the garnet peridotite. They are (1) rutile, (2) orthopyroxene, and (3) clinopyroxene. Back-scattered electron (BSE) images with the assistance of Photoshop 6.0 were used to estimate volume abundances of the exsolved phases.

Figure 3 shows abundant rutile lamellae exsolved from the porphyroblastic garnet host of sample 2C42 and 2C28. The rutile lamellae are needles up to 500 µm long (Figs. 3a–3c) with basal sections 0.5–3 µm (up to 5 µm) in diameter. BSE images show that this garnet grain locally contains up to 1.0 vol% rutile rods with an average of about 0.6 vol%. Detailed petrography reveals that about half the rutile needles exhibit oblique extinction, which, as seen elsewhere (van Roermund 2000), is thought to be possible high-pressure rutile polymorphs (van Roermund, pers. comm. 2003). The rutile needles always occur in association with and locally intergrown with other silicate exsolution lamellae as described below.

Pyroxene lamellae (up to 0.8 vol%) occur in close association with rutile needles in garnets from samples 2C28. They are spindle-shaped in the long section and hexagonal in the basal section (Figs. 3b). The amount of the pyroxene lamellae varies in different garnet grains, but is up to 4.5 vol% in the BSE images (Fig. 3d). Pyroxene lamellae were also observed in garnets from sample 2C42; they occur as hexagonal prismatic crystals in association with rutile with their crystal planes parallel to the three directions of the rutile rods (Fig. 3c). Orthopyroxene (dark phase) and clinopyroxene (pale-grey phase) lamellae can be readily distinguished on BSE images (Fig. 3d) and by electron probe microanalysis (Table 1).

All these exsolution lamellae occur in parallel groups, each being strictly oriented in one of the four directions corresponding to the isometric form {111} (i.e., octahedral planes), which form a distinct equilateral triangle pattern in Figure 3a. The high abundances and regular distributions with respect to crystallographic axes/planes suggest that the rods of rutile and pyroxene in porphyroblastic garnets were generated by decompression-induced exsolution, rather than by epitaxial replacement or accidental inclusion.

Table 1 gives representative compositions of both matrix

TABLE 1. Compositions of matrix minerals and exsolved lamellae in garnet peridotites

	Matrix								Exsolution lamellae				C-O
Sample	2C42 Grt	2C42 Opx	2C42 Cpx	2C42 Ol	2C28 Grt	2C28 Opx	2C28 Cpx	2C28 Ol	2C28 Cpx	2C28 Opx	2C42 Opx	2C42 Ilm	2C28 Grt
							Wt% oxides						
SiO_2	42.11	57.82	55.13	40.60	41.90	56.94	54.19	40.15	54.18±0.18	57.03±0.39	57.54±0.51	0.02	42.20
TiO_2	0.18	0.09	0.23	0.00	0.04	0.05	0.24	0.00	0.53±0.05	0.03±0.02	0.03±0.03	58.67	0.85
Al_2O_3	22.31	0.38	3.19	0.00	22.78	0.50	2.23	0.01	4.14±0.13	0.82±0.15	1.13±0.24	0.00	21.67
Cr_2O_3	1.44	0.15	1.26	0.04	0.62	0.26	1.75	0.05	1.36±0.16	0.19±0.04	0.19±0.01	0.12	0.62
FeO	9.69	5.52	1.75	9.31	10.52	6.34	0.63	8.60	1.70±0.18	6.16±0.17	6.26±0.58	33.38	10.13
MnO	0.43	0.11	0.07	0.10	0.44	0.16	0.00	0.05	0.06±0.04	0.13±0.04	0.18±0.01	0.44	0.42
NiO	0.03	0.08	0.04	0.36	0.00	0.08	0.03	0.28	0.05±0.03	0.05±0.02	0.01±0.01	0.17	0.00
MgO	19.57	35.78	15.76	50.54	19.33	34.76	16.73	50.11	15.68±0.21	34.71±0.41	34.81±0.31	8.72	19.44
CaO	4.33	0.20	21.32	0.00	4.06	0.24	23.49	0.11	19.97±0.36	0.23±0.03	0.16±0.06	0.01	4.31
Na_2O	0.04	0.01	1.38	0.03	0.01	0.00	0.91	0.00	2.10±0.15	0.00±0.00	0.00±0.00	0.02	0.06
K_2O	0.01	0.01	0.00	0.00	0.00	0.00	0.00	0.01	0.01±0.01	0.00±0.00	0.00±0.00	0.01	0.00
Total	100.13	100.15	100.13	100.98	99.70	99.33	100.20	99.37	99.95±0.34	99.33±0.19	100.29±0.20	101.56	99.70
							Cations						
O	12	6	6	4	12	6	6	4	6	6	6	6	12
Si	3.008	1.980	1.981	0.986	3.007	1.978	1.955	0.987	1.952±0.012	1.977±0.011	1.975±0.013	0.001	3.029
Ti	0.009	0.001	0.006	0.000	0.002	0.001	0.007	0.000	0.014±0.002	0.001±0.001	0.001±0.000	2.038	0.046
Al	1.879	0.019	0.135	0.000	1.927	0.021	0.095	0.000	0.176±0.003	0.034±0.006	0.046±0.010	0.000	1.833
Cr	0.081	0.008	0.036	0.001	0.035	0.007	0.018	0.000	0.039±0.004	0.005±0.001	0.005±0.000	0.004	0.035
Fe^{2+}	0.579	1.790	0.053	0.189	0.631	0.184	0.054	0.177	0.051±0.005	0.179±0.002	0.180±0.017	1.289	0.608
Mn	0.026	0.015	0.002	0.002	0.027	0.005	0.000	0.001	0.002±0.001	0.004±0.001	0.005±0.000	0.017	0.026
Ni	0.002	0.006	0.001	0.007	0.000	0.002	0.001	1.837	0.001±0.001	0.001±0.000	0.000±0.000	0.006	0.000
Mg	2.084	0.003	0.844	1.829	2.068	1.800	0.900	0.003	0.842±0.005	1.794±0.020	1.781±0.021	0.601	2.080
Ca	0.331	0.185	0.821	0.000	0.312	0.009	0.908	0.000	0.770±0.002	0.008±0.001	0.006±0.002	0.000	0.331
Na	0.004	0.001	0.096	0.001	0.001	0.000	0.064	0.000	0.160±0.009	0.000±0.000	0.000±0.000	0.002	0.009
K	0.001	0.000	0.000	0.000	0.000	0.000	0.000	0.006	0.000±0.000	0.000±0.000	0.000±0.000	0.001	0.000
Total	8.005	4.007	3.975	3.015	8.011	4.007	4.002	3.011	4.007±0.010	4.003±0.008	3.999±0.017	3.960	7.996

Notes: Abbreviations: Grt = garnet; Opx = orthopyroxene; Cpx = clinopyroxene; Ol = olivine; Ilm = ilmenite; C-O = calculated original garnet. The original composition of garnet in 2C28 is calculated from 94.7% averaged garnet plus 0.8 % TiO_2, 4.5% averaged pyroxene exsolutions. Analytical errors in matrix minerals are < ± 2% for SiO_2, Al_2O_3, FeO, MgO and CaO (except olivine and orthopyroxene), for TiO_2, Cr_2O_3 and MnO < ± 10%, and Na_2O, > ± 20% for garnet, olivine, orthopyroxene but greater than ±10% for clinopyroxene. Errors of exsolution lamellae are 1σ.

host minerals and exsolution lamellae analyzed using a JEOL JXA-8100 Electron Probe Microanalyzer at Peking University. Analytical conditions were optimized for standard silicates and oxides at 15 kV accelerating voltage, with 20 nA beam current and an ~1 μm beam spot for all the elements. Routine analyses were obtained by counting for 20 seconds at peak and 5 seconds on background. Repeated analysis of natural and synthetic mineral standards yielded precisions better than ±2% for most elements.

Garnet grains in all types of rocks are fairly homogeneous without obvious core-rim zoning. High concentrations of TiO_2 (0.16–0.20 wt%) and Na_2O (up to 0.08 wt% with an average of 0.04 wt%) have been detected in matrix porphyroblastic garnets (Table 1). Exsolved orthopyroxene rods contain slightly higher Al_2O_3 (0.9–1.2 wt%) than the matrix orthopyroxene. Exsolved clinopyroxene rods, on the other hand, contain higher jadeite component (X_{Jd} = 0.14) than the matrix clinopyroxene (X_{Jd} = 0.03–0.10). Based on the estimated amount and compositions of various exsolution lamellae, we have calculated the original (prior to exsolution) garnet composition 2C28 (see Table 1 note for calculation procedure). Compositions of the majoritic garnet may be defined by four end-members: $Mg_3Al_2Si_3O_{12}$, $Ca_2Na(SiAl)Si_3O_{12}$, $M_3(MTi)Si_3O_{12}$, and $M_3(MSi)Si_3O_{12}$ (Zhang and Liou 2003). The precursor garnet for this sample contains 0.9% $Ca_2Na(SiAl)Si_3O_{12}$, 2.0% $M_3(MSi)Si_3O_{12}$, 4.6% $M_3(MTi)Si_3O_{12}$, and 92.4% $Mg_3Al(+Cr)_2Si_3O_{12}$.

ILMENITE AND AL-CHROMITE PRECIPITATES IN OLIVINE

Ilmenite [$(Fe,Mg)TiO_3$] rods are abundant in the first generation of large olivine crystals from the garnet peridotite. These rods are well oriented, densely and homogeneously packed, and parallel to [010] of the olivine host (Figs. 4a and 4c). The rods are 20–100 μm in length and 0.3–1.5 μm in width/thickness. Some rods are up to 3 μm in diameter in their basal sections, which allows precise analysis of their compositions unaffected by the host olivine. Concentrations of the ilmenite rods vary in different grains as well as in different samples; BSE images show that the ilmenite exsolutions in some host olivines make up to ~1.18% (Fig. 4b) and 0.92% (Fig. 4c) of the total surface area. This result suggests that the olivine can have as much as 0.69 wt% and 0.53 wt% TiO_2, respectively. Compositional analyses show that these ilmenite rods are characterized by high TiO_2 (58.7–59.2 wt%) and MgO (8.7–12.4 wt%) (Table 1), which yields the following structural formula: $(Na_{0.001}Fe_{0.645}Mg_{0.300}Ni_{0.005}Mn_{0.010})Ti_{1.02}O_3$.

Needle-like Al-chromite precipitates are also found in the first generation of large olivine grains from the garnet peridotite. They occur either in individual olivines or in association with ilmenite rods. In contrast to the ilmenite rods, Most Al-chromite needles are long (50–300 μm) but too thin (~1 μm) to be analyzed properly (Figs. 4e and 4f). Figure 4e shows that Al-chromite needles occur in four groups of directions: one major group is parallel to the olivine [010]: one group parallel to [001] as dotted points on the (001) plane, and the other two groups intersect the [010] rods with a ~60° angle between the two groups. We also observed the [001] group of Al-chromite rods perpendicular to [010] ilmenite rods (Fig. 4c). A BSE image (Fig. 4f) shows that Al-chromite needles can amount to 0.6 vol% in some olivine grains. An EDS (energy dispersive spectrometer) spectrum (inset of Fig. 4f) shows that these needles have strong Al and Cr peaks,

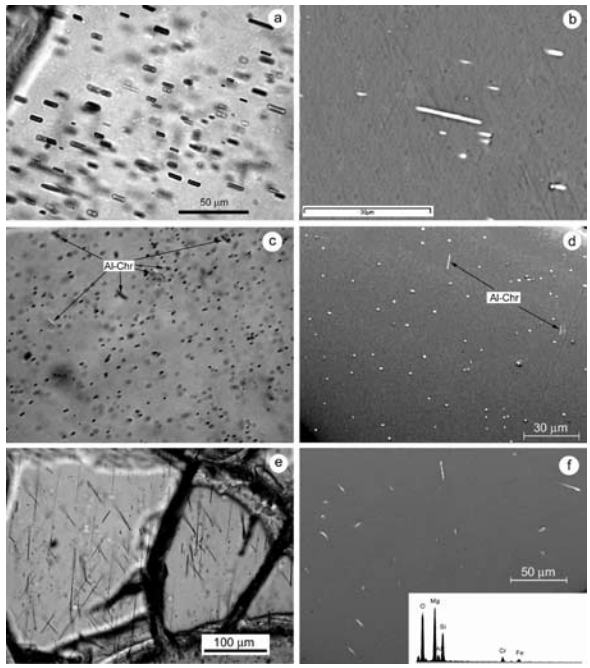

FIGURE 4. Photomicrographs of Cr-spinel and ilmenite precipitates in olivines from garnet peridotite. (**a**) Image of ilmenite precipitates in olivine in sample 2C28 (plane-polarized transmitted light). (**b**) BSE image of ilmenite rods in sample 2C28. (**c**) Image of ilmenite and Cr-spinel precipitates in olivine of sample 2C42 (plane-polarized transmitted light). (**d**) BSE image of c. (**e**) Four oriented groups of Cr-spinel rods in olivine of sample 2C38 (plane-polarized transmitted light). (**f**) BSE image of e with accompanying EDS spectrum in the insert.

but relatively weak Fe peak. The structural formula of the Al-chromite is $(Mg,Fe)(Cr,Al)_2O_4$.

DISCUSSION

Ultrahigh-pressure origin—evidence from garnet exsolutions

We have identified three different exsolution lamellae in garnets from the Luliangshan garnet peridotite, North Qaidam. These are rutile, orthopyroxene, and clinopyroxene. The orientation of these needles and their topotaxial relationships with the host garnet suggest that all these needles are exsolution phases from their parental garnet rather than trapped or replaced inclusions.

Supersilicic garnet, majorite or majoritic garnet, is a rare mineral that occurs in nature (e.g., Ringwood et al. 1992) but has been well-demonstrated experimentally to be stable at pressures in excess of 5 GPa (Ringwood and Major 1971; Akaogi and Akimoto 1977; Irifune 1987; Irifune et al. 1994). Pyroxene exsolutions from garnets provide direct evidence for the existence of majoritic garnets in rocks from UHP belts, which has been interpreted as a crucial indication of continental subduction to, and exhumation from, the mantle at depths greater than 180 to 200 km (van Roermund and Drury 1998; Ye et al. 2000). Under UHP conditions, garnet becomes Al-deficient and deviates from normal garnet stoichiometry (Moore and Gurney 1985). In this case, dissolution of pyroxene into garnet requires excess Si to reside in octahedral sites to replace Al^{3+} (+ Cr^{3+}) in converted majoritic garnet. This transformation can be expressed by the coupled substitution of ^{VI}Mg (or Ca) + $^{VI}Si \rightarrow 2^{VI}Al$ and ^{VIII}Na + $^{VI}Si \rightarrow {}^{VIII}Ca + {}^{VI}Al$ (Sobolev et al. 1971).

Experimental studies have also shown that garnet can contain high Ti, Na, and P contents under very high pressures (Ringwood and Lovering 1970; Tompsom 1975; Zhang et al. 2003), which explains the close association of abundant TiO_2 lamellae with exsolutions of Na-rich clinopyroxene in our samples. Experimental studies and field observations demonstrate that with increasing pressure, the solubility of pyroxene in garnet increases (Irifune et al. 1986; Ono and Yasuda 1996), and Ti (including Na and P) concentrations in garnet also display a positive pressure dependence (Tompsom 1975, Zhang et al. 2003). The high concentrations of rutile (about 1.0 vol%) and pyroxene exsolutions suggests the existence of a $(Ca_2Na)(AlTi)Si_3O_{12}$ component in the precursor garnet crystals, which may arise through the substitution Ti + Na → Al + Ca and Mg (or Ca) + Ti → 2Al at ultrahigh pressures.

As expected, the Ti (including Na and P) content in the bulk Mg-Cr-type garnet peridotite is much lower than those in eclogites metamorphosed from basaltic rocks (e.g., MORB and OIB) and in garnet peridotite from Fe-Ti-type cumulate intrusions. Considering the high amount of pyroxene exsolutions (up to 4.5 vol%) and octahedral Si + Ti contents in the original garnet plus all the above observations, we conclude that the original garnet or majoritic garnet from garnet peridotite in the North Qaidam UHP belt may have been formed at pressures about 7 GPa. That is, the garnet peridotite body may have been exhumed from mantle depths in excess of 200 km.

Ultrahigh-pressure origin—evidence from olivine exsolutions

Ilmenite and chromite precipitates in olivines were described by Dobrzhinetskaya et al. (1996) from the Alpe Arami massif. From TEM electron diffraction patterns, these authors suggested that the $(Fe,Mg)TiO_3$ rods have three different structures previously unrecognized. They proposed that the originally unexsolved phase was the high-pressure perovskite-structured polymorph of ilmenite formed at a minimum depth of 300 kilometers or even in the transition zone (i.e., 410–660 km) (Green et al. 1997b), where the olivine may then be wadsleyite. $FeTiO_3$ exsolution rods also have been reported in olivines from the Chaijiadian garnet lherzolite, Sulu UHP terrane of eastern China (Hacker et al. 1997). The interpreted ultra-deep origin of these peridotites has triggered some heated debates on their tectonic implications in recent years (Hacker et al. 1997; Pfiffner and Trommsdorff 1998; Trommsdorff et al. 2000; Risold et al. 2001). The more-recent discovery of high-pressure C2/c clinoenstatite (Bozhilov et al. 1999) in the Alpe Arami peridotites lends strong support for their ultra-deep origin and exhumation from a minimum depth of 250 km.

Titanium, Cr, Al and Fe^{3+} are trace metals usually unmeasured in olivines. Dobrzhinetskaya et al. (1999) showed experimentally that the solubility of TiO_2 in olivines increases markedly with increasing pressure and temperature. TiO_2 in olivine was undetected at 5 GPa and 1400 K. With increasing pressure from 8 to 12 GPa and temperature from 1400 to 1700 K, TiO_2 content in olivines increases from 0.4 to > 1.0 wt%. Tinker and Lesher (2001) concluded from their experiments that olivine containing 0.6 wt% TiO_2 may have originated from depths of > 300 km (>10 GPa). Our observation of 0.92–1.18 vol% $(Fe, Mg)TiO_3$ exsolu-

tion lamellae (corresponding to 0.53–0.69 wt% TiO_2) in olivine indeed points to very high-Ti precursor olivine in the garnet peridotite of this study, which perhaps can be explained only by the ultra-high pressure (>7 GPa) origin of the original olivine. The significant amount of geikielite ($MgTiO_3$) component in the ilmenite rods suggests Mg substitution for Fe in ilmenite is expected at high pressures (Bozhilov et al. 2003).

Furthermore, the densely packed Al-chromite rods (up to 0.6 vol%) suggest that some of the first generation of olivines originally were rich in Cr and Al. The four groups of oriented Al-chromite needles imply that the original structure of the host olivine may have been spinelloid (wadsleyite-type). Olivine-wadsleyite transformation experiments have demonstrated that trivalent cations such as Cr and Al can be stored better in wadsleyite (β-olivine) structures with a coupled substitution of 2Cr (+ Al) for Mg + Si at very high pressures (Gudfinnsson and Wood 1998). Al-chromite precipitates with similar composition also have been observed in olivine inclusions in diamond, which are believed to be exsolved products during the phase transformation of wadsleyite to olivine (Brenker et al. 2002). These observations in olivines, taken together with evidence from garnet exsolutions discussed above, strongly suggest that the garnet peridotite originated at depths greater than 7 GPa.

P-T Path of the garnet peridotite

With the recognition of relict Ti-rich majoritic garnet, the garnet peridotite in the North Qaidam UHP belt can be traced back to origination depths >200 km. High concentrations of ilmenite and Al-Chromite exsolutions in the first generation of coarse-grained olivines suggest originally high Ti-Cr-Al compositions, and also imply possible higher pressure conditions at greater than 7 GPa based on experiments for solubility of TiO_2 in olivine (Dobrzhinetskaya et al. 1999; Tinker and Lesher 2001). On the other hand, application of Al-in-Opx geothermobarometer of Brey and Köhler (1990) and Grt-Ol geothermometer of O'Neill et al. (1979) to matrix-host minerals (Table 1) in the garnet peridotite yields P = 5.0–6.5 GPa and T = 960–1040 °C, and, in garnet-bearing dunite, P = 4.6–5.3 GPa and T = 980–1130 °C. This calculated pressure range, if reliable, can only represent the minimum values because of the subsequent re-equilibration during exhumation (e.g., exsolution effects). Using the Al-in-Opx geobarometer and the two-pyroxene thermometer (Brey and Köhler 1990), we obtained *P-T* conditions for the vein-like garnet pyroxenite as P = 3–3.5 GPa and T = 850–950 °C, which are obviously lower than that of garnet-lherzolite and garnet-bearing dunite. Thus, based on the P-T evolution of the garnet peridotite, we suggest the following multistage exhumation history for the North Qaidam garnet peridotite, as shown in Figure 5: Stage I, origin and metamorphism at depths greater than 200 km within a subduction zone (although its ultimate petrogenesis is beyond the scope of current study); Stage II, uplift with the UHP continental crust and re-equilibration at depths of 3–3.5 GPa (about 100 km) where the vein-like garnet pyroxenite forms; and Stage III, exhumation to the upper crustal levels during which garnets break down to a symplectite of clinopyroxene + orthopyroxene + spinel.

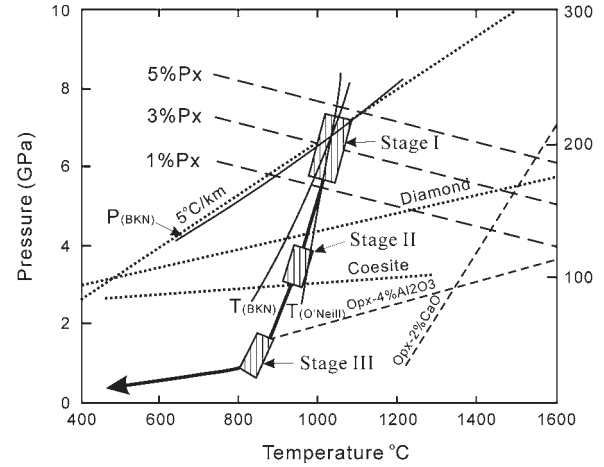

FIGURE 5. *P-T* path of the Luliangshan garnet peridotite. Stage I: *P-T* estimates from exsolutions in garnets and olivines and from geothermobarometric calculations of matrix minerals of sample 2C42 and 2C28. Stage II: *P-T* estimates from geothermobarometric calculations of matrix mineral of vein-like garnet pyroxenite. Stage III: *P-T* estimates from breakdown of garnets into kelyphitic Cpx + Opx + Spl ± Amp. $T_{(BKN)}$ and $P_{(BKN)}$ are temperature and pressure curves calculated by geothermobarometer of Brey and Köhler (1990), and $T_{(O'Neill)}$ is temperature curve by Grt–Ol geothermometer of O'Neill and Wood (1979). The lines labeled 1, 3, and 5% Px are isopleths of pyroxene dissolved in garnet (after von Roermund et al. 2001).

ACKNOWLEDGMENTS

This study was financially supported by Major State Basic Research Development Projects (G1999075508), National Natural Science Foundation of China (grants nos. 40272031, 40228003, 40372031, 40325005) and Chinese Post-doc Foundation to S.G.S. C.J. Wei and Y.F. Zhu are thanked for discussion. Microprobe work benefited from help of G.M. Su. G.P. Brey and J.J. Yang are thanked for providing *P-T* calculation programs and S.-s. Sun, J.G. Liou and J.J. Yang for critical review and their help in improving quality of the manuscript. We also thank H. van Roermund and H-J. Massonne for their constructive journal review comments and J.G. Liou for his final improvements.

REFERENCES CITED

Akaogi, M. and Akimoto, S. (1977) Pyroxene-garnet solid solution equilibria in the systems $Mg_4Si_4O_{12}$-$Mg_3Al_2Si_3O_{12}$ and $Fe_4Si_4O_{12}$-$Re_3Al_2Si_3O_{12}$ at high pressures and temperatures. Physics of the Earth and Planetary Interiors, 15, 90–106.

Bozhilov, K.N., Green II, H.W., and Dobrzhinetskaya, L. (1999) Clinoenstatite in Alpe Arami peridotite: additional evidence of very high pressure. Science, 284, 128–132.

——— (2003) Quantitative 3D measurement of ilmenite abundance in Alpe Arami olivine by confocal microscopy: Confirmation of high-pressure origin. American Mineralogist, 86, 596–603.

Brenker, F.E., Stachel, T., and Harris, J. W. (2002) Exhumation of lower mantle inclusions in diamond: ATEM investigation of retrograde phase transitions reactions and exsolution. Earth and Planetary Science Letters, 198, 1–9.

Brey, G.P. and Köhler, T. (1990) Geothermobarometry in four-phase lherzolites. Part II: New thermobarometers, andpractical assessment of existing thermobarometers. Journal of Petrology, 31, 1353–1378.

Brueckner, H.K. and Medaris, L.G. (2000) A general model for the intrusion and evolution of 'mantle' garnet peridotites in high-pressure and ultra-high-pressure metamorphic terranes. Journal of Metamorphic Geology, 18, 123–133. {auth: citation not found in text, please insert or delete from list?}

Bureau of Geology and Mineral Resources of Qinghai Province (1991) Regional geology of Qinghai Province. Geological Memoirs of Ministry of Geology and Mineral Resources, People's Republic of China, Series 1, Number 24, p. 1–661, Geological Publishing House, Beijing.

Dobrzhinetskaya, L., Green, H.W., and Wang, S. (1996) Alpe Arami: a peridotite massif from depths of more than 300 kilometers. Science, 271, 1841–1845.

Dobrzhinetskaya, L., Bozhilov, K.N., and Green II, H.W. (1999) The solubility of TiO_2 in olivine: implications for the mantle wedge environment. Chemical Geology, 160, 357–370.

Ernst, G. (2001) Subduction, ultrahigh-pressure metamorphism, and regurgitation of buoyant crustal slices—implications for arcs and continental growth. Physics of the Earth and Planetary Interiors, 127, 253–275.

Green II, H.W., Dobrzhinetskaya, L., Riggs, E., and Jin, Z.-M. (1997) Alpe Arami: a peridotite massif from the mantle transition zone? Tectonophysics, 279, 1–21.

Gudfinnsson, G.H. and Wood, B.J. (1998) The effect of trace elements on the olivine-wadsleyite transformation. American Mineralogist, 83, 1037–1044.

Hacker, B., Sharp, T., Zhang, R.Y., Liou, J.G., and Hervig, R.L. (1997) Determining the origin of ultrahigh-pressure lherzolites (discussion). Science, 278, 702–704.

Haggerty, S.E. and Sautter, V. (1990) Ultradeep (greater than 300 kilometers), ultramafic upper mantle xenoliths. Science, 248, 993–996. {auth: not cited in paper, please add or delete from list}

Irifune, T., Sekine, T., Ringwood, A.E. and Hibberson, W.O. (1986) The eclogite garnet transformation at high pressure and some geographical implications. Earth and Planetary Science Letters, 77, 245–256.

Irifune, T. (1987) An experimental investigation of the pyroxene-garnet transformation in a pyrolite composition and its bearing on the constitution of the mantle. Physics of the Earth and Planetary Interiors, 45, 324–336.

Irifune, T., Hibberson, W.O., and Ringwood, A.E. (1994) Eclogite-garnetite transformation at high pressure and its bearing on the occurrence of garnet inclusions in diamond. In J. Ross, Ed., Kimberlites and Related Rocks, p. 877–882. Blackwell, Melburne.

Kretz, R. (1983) Symbols for rock-forming minerals. American Mineralogist, 68, 277–279.

Liou, J.G. and Carswell, D.A. (2000) Preface: Garnet Peridotites and Ultrahigh-Pressure Minerals. Journal of Metamorphic Geology, 18, 121.

Massonne, H-J. and Bautsch, H-J. (2002) An unusual garnet pyroxenite from the Granulitgebirge, Germeny: origin in the Transition Zone (>400 km depths) or in a shallower upper mantle region? International Geology Review, 44, 779–796.

Medaris, L.M. and Carswell, D.A. (1990) Petrogenesis of Mg-Cr garnet peridotites in European metamorphic belts. In D.A. Carswell, Ed., Eclogite Facies Rocks, p. 260–291. Blackie, Glasgow.

Moore, R.O. and Gurney, J.J. (1985) Pyroxene solid solution in garnets included in diamond. Nature, 318, 553–555.

O'Neill, H.St.-C. and Wood, B.J. (1979) An experimental study of Fe-Mg-partitioning between garnet and olivine and its calibration as a geothermometer. Contributions to Mineralogy and Petrology, 70, 59–70.

Ono, S. and Yasuda, A. (1996) Compositional change of majoritic garnet in a MORB composition from 7 to 17 GPa and 1400 to 1600 °C. Physics of the Earth and Planetary Interiors, 96, 171–179.

Pfiffner, M. and Trommsdor, V. (1998) The high-pressure ultramafic-mafic-carbonate suite of Cima Lunga-Adula, Central Alps: excursions to Cima di Gagnone and Alpe Arami. Schweizerische Mineralogische und Petrographische Mitteilungen, 8, 337–354.

Ringwood, A.E. and Lovering, J.F. (1970) Significance of pyroxene-ilmenite intergrowths among kimberlite xenoliths. Earth and Planetary Science Letters, 7, 371–375.

Ringwood, A.E. and Major, A. (1971) Synthesis of majorite and other high pressure garnets and perovskites. Earth and Planetary Science Letters, 12, 411–418.

Ringwood, A.E., Kesson, S.E., Hibberson, W., and Ware, N. (1992) Origin of kimberlites and related magmas. Earth and Planetary Science Letters, 113, 521–538.

Risold, A.-C, Trommsdorff, V., and Grobety, B. (2001) Genesis of ilmenite rods and palisades along humite-type defects in olivine from Alpe Arami. Contributions to Mineralogy and Petrology, 140, 619–628.

Smith, D. (1999) Temperatures and pressures of mineral equilibration in peridotite xenoliths: Review, discussion, and implications. In Y. Fei, C.M. Bertka, and B.O., B.O. Mysen, Eds., Mantle Petrology: Field Observations and High Pressure Experimentation, Geochemical Society Special Publication, 6, 171–188. Geochemical Society, St. Louis, MO.

Sobolev, N.V., Lavrent'ev, G., and Yu, G. (1971) Isomorphic sodium admixture in garnets formed at high pressure. Contributions to Mineralogy and Petrology, 31, 1–12.

Song, S.G. (1996) Metamorphic Geology of Blueschists, Eclogites and Ophiolites in the North Qilian Mountains. 30th IGC Field Trip Guide T392, 40p, Geological Publishing House, Beijing.

——— (2001) Petrology, Mineralogy and Metamorphic Evolution of the Dulan UHP Terrane in the North Qaidam, NW China and Its Tectonic Implications. Doctoral Thesis, Chinese Academy of Geological Science, Beijing (in Chinese).

Song, S.G., Yang, J.S., Xu, Z.Q., Liou, J.G., and Shi, R.D. (2003a) Metamorphic Evolution of the Coesite-bearing Ultrahigh-pressure Terrane in the North Qaidam, northern Tibet, NW China. Journal of Metamorphic Geology, 21, 631–644.

Song, S.G., Yang, J.S., Liou, J.G., Wu, C.L., Shi, R.D., and Xu, Z.Q. (2003b) Petrology, Geochemistry and isotopic ages of eclogites in the Dulan UHPM terrane, the North Qaidam, NW China. Lithos, 70, 195–211.

Tinker, D. and Lesher, C.E. (2001) Solubility of TiO_2 in Olivine from 1 to 8 GPa. EOS Transition of the American Geophysical Union 82, Fall Meeting Supplement, Abstract no. V51B-1001.

Tompsom, R.N. (1975) Is upper-mantle phosphorus contained in sodic garnet? Earth and Planetary Science Letters, 26, 417–424.

Trommsdorff, V., Hermann, J., Müntener, O., Pfiffner, M., and Risold, A.-C (2000) Geodynamic cycles of subcontinental lithosphere in the Central Alps and the Arami enigma. Journal of Geodynamics, 30, 77–92.

van Roermund, H.L.M. and Drury, M.R. (1998) Ultra-high pressure (P > 6 GPa) garnet peridotites in Western Norway: exhumation of mantle rocks from >185 km depth. Terra Nova, 10, 295–301.

van Roermund, H.L.M., Drury, M.R., Barnhoorn, A., and de Ronde, A. (2000) Super-silicic garnet microstructures from an orogenic garnet peridotite, evidence for an ultra-deep (>6 GPa) origin. Journal Metamorphic Geology, 18, 135–147.

van Roermund, H.L.M., Drury, M.R., Barnhoorn, A., and de Ronde, A. (2001) Non-silicate inclusions in garnet from an ultra-deep orogenic peridotite. Geological Journal, 35, 209–229.

van Roermund, H.L.M., Carswell, D.A., Drury, M.R., and Herjboer, T.C. (2002) Microdiamonds in a megacrystic garnet websterite pod from Bardane on the island of Fjørtoft, western Norway: Evidence for diamond formation in mantle rocks during deep continental subduction. Geology, 30, 959–962.

Wu, H.Q., Feng, Y.M., and Song, S.G. (1993) Metamorphism and deformation of blueschist belts and their tectonic implications, North Qilian Mountains, China. Journal of Metamorphic Geology, 11, 523–536.

Yang, J.J., Godard, G., Kienast, J.R., Lu, Y., and Sun, J. (1993) Ultrahigh-pressure (60 kbar) magnesite-bearing garnet peridotites from northeastern Jiangsu, China. J. Geol. {auth: Journal name MUST be spell out}101, 541–554.

Yang, J.J., Zhu, H., Deng, J.F., Zhou, T.Z., and Lai, S.C. (1994) Discovery of garnet-peridotite at the northern margin of the Qaidam Basin and its significance. Acta Petrologica et Mineralogica, 13, 97–105 (in Chinese with English abstract).

Yang, J.S., Xu, Z.Q., Song, S.G., Zhang, J.X., Wu, C.L., Shi, R.D., Li, H.B., Brunel, M., and Tapponnier, P. (2002) Subduction of continental crust in the early Paleozoic North Qaidam ultrahigh-pressure metamorphism belt, NW China: Evidence from the discovery of coesite in the belt. Acta Geologica Sinica, 76, 63–68.

Ye, K., Cong, B., and Ye, D. (2000) The possible subduction of continental material to depths greater than 200 km. Nature, 407, 734–736.

Zhang, J.X., Yang, J.S., Xu, Z.Q., Zhang, Z.M., Chen, W., and Li, H.B. (2000) Peak and retrograde age of eclogites at the northern margin of Qaidam basin, Northwestern China: evidences from U-Pb and Ar-Ar dates. Geochemica, 29, 217–222 (in Chinese with English abstract).

Zhang, R.Y. and Liou, J.G. (1999) Exsolution lamellae in minerals from ultrahigh-P rocks. International Geology Review, 41, 981–993.

Zhang, R.Y. and Liou, J.G. (2003) Clinopyroxenite from the Sulu ultrahigh-pressure terrane, eastern China: Origin and evolution of garnet exsolution in clinopyroxene. American Mineralogist, 88, 1591–1600.

Zhang, R.Y., Liou, J.G., and Yang, J.S. (2000) Petrochemical constraints for dual origin of garnet peridotites of the Dabie-Sulu UHP terrane, China. Journal of Metamorphic Geology, 18, 149–166.

Zhang, R.Y., Zhai, S.M., Fei, Y.W., and Liou, J.G. (2003) Titaniun solubility in coexisting garnet and clinopyroxene at very high pressure: the significance of exsolved rutile in garnet. Earth and Planetary Science Letters, 216, 591–601.

MANUSCRIPT RECEIVED APRIL 3, 2003
MANUSCRIPT ACCEPTED MARCH 18, 2004
MANUSCRIPT HANDLED BY J. LIOU